

# Quasiparticles in the superconducting state of $Bi_2Sr_2CaCu_2O_{8+\delta}$

A. Kaminski,<sup>1</sup> J. Mesot,<sup>2</sup> H. Fretwell,<sup>1</sup> J. C. Campuzano,<sup>1,2</sup> M. R. Norman,<sup>2</sup> M. Randeria,<sup>3</sup> H. Ding,<sup>4</sup> T. Sato,<sup>5</sup> T. Takahashi,<sup>5</sup> T. Mochiku,<sup>6</sup> K. Kadokawa,<sup>7</sup> and H. Hoechst<sup>8</sup>

(1) Department of Physics, University of Illinois at Chicago, Chicago, IL 60607

(2) Materials Science Division, Argonne National Laboratory, Argonne, IL 60439

(3) Tata Institute of Fundamental Research, Mumbai 400005, India

(4) Department of Physics, Boston College, Chestnut Hill, MA 02467

(5) Department of Physics, Tohoku University, 980-8578 Sendai, Japan

(6) National Research Institute for Metals, Sengen, Tsukuba, Ibaraki 305, Japan

(7) Institute of Materials Science, University of Tsukuba, Ibaraki 305, Japan

(8) Synchrotron Radiation Center, Stoughton, WI, 53589

Recent improvements in momentum resolution by a factor of 32 lead to qualitatively new ARPES results on the spectra of  $Bi_2Sr_2CaCu_2O_{8+\delta}$  (Bi2212) along the  $(\pi, \pi)$  direction, where there is a node in the superconducting gap. With improved resolution, we now see the intrinsic lineshape, which indicates the presence of true quasiparticles at the Fermi momentum in the superconducting state, and lack thereof in the normal state. The region of momentum space probed here is relevant for charge transport, motivating a comparison of our results to conductivity measurements by infrared reflectivity.

71.25.Hc, 74.25.Jb, 74.72.Hs, 79.60.Bm

Landau's concept of the Fermi liquid [1] underlies much of our present theoretical understanding of electron dynamics in crystalline solids. Landau was able to demonstrate that, even though the electrons interact strongly with one another, one can still describe the low temperature properties of metals in terms of "quasiparticle" excitations, which are bare electrons dressed by the medium in which they move. But we now have materials, such as the high temperature superconductors (HTSCs), and other low dimensional systems, where it is becoming increasingly difficult to reconcile experimental results with the expectations of Fermi liquid theory [2,3].

Clearly, if the concept of quasiparticles is to be useful, they must live long enough to be considered as independent entities. In fact, in a Fermi liquid, the quasiparticles at the Fermi momentum,  $k_F$ , have (at zero temperature) an infinite lifetime at zero excitation energy - the Fermi energy,  $E_F$  - with their lifetime decreasing quadratically with excitation energy [1]. If one were to measure the spectral function of the electrons at  $k_F$ , one would observe a broad feature, corresponding to the incoherent part of the electron, with a sharp peak at  $E_F$  with spectral weight  $z$ , the quasiparticle component. It is now well established by angle resolved photoemission spectroscopy (ARPES) measurements that, despite the existence of a Fermi surface in momentum space, there are no quasiparticles in the normal state of optimally doped or slightly overdoped HTSCs near the  $(\pi, 0)$  point of the Brillouin zone (see inset of Fig. 1) [4,5]. Below  $T_c$ , the superconducting gap is maximal here (at the anti-node point  $A$ ) and sharp quasiparticle peaks are observed [6]. This statement can be made since the energy dispersion of the electronic states in this region of the zone is very weak, and therefore the measured spectra are not artifi-

cially broadened by the finite acceptance angle (momentum window) of the detector.

Along the zone diagonal, however, the intrinsic lineshape is unknown, both in the normal and superconducting states, because the spectra near point N (at the Fermi surface along the diagonal; see inset of Fig. 1) are significantly broadened by the momentum window given the highly dispersive nature (1.6 eVÅ) of the states in this region. This observation is reinforced by the lack of any temperature dependence of the spectra at point N in sharp contrast to what is observed at point A. In this work, a large improvement in experimental momentum resolution allows us to determine the intrinsic lineshape at  $N$  for the first time. The significance of these observations stems from the fact that this region of the zone dominates many of the bulk properties of cuprate superconductors, and it is very important to know if and when quasiparticles exist. Above  $T_c$ , the charge and thermal transport are dominated by these states because of their rapid dispersion (large Fermi velocity). Below  $T_c$ , the superconducting energy gap vanishes at the nodal point  $N$ , and low energy excitations in its neighborhood dominate the  $T$ -dependence of various properties, e.g., the superfluid density [7].

ARPES gives direct information about the momentum and energy dependence of the lifetime of electrons, since it probes the spectral function whose width is controlled by this lifetime. In quasi-2D materials, the ARPES signal is given by [6]  $I(\omega) = I_{\mathbf{k}} f(\omega) A(\mathbf{k}, \omega)$ , where  $I_{\mathbf{k}}$  is the dipole matrix element between initial and final states,  $f(\omega)$  the Fermi function, and the spectral function  $A(\mathbf{k}, \omega)$  is the probability of adding or removing an electron with momentum  $\mathbf{k}$  and energy  $\omega$  from the system. Curve (a) in the bottom left panel of Fig. 1 shows an

ARPES spectrum in the normal state at 100K for an optimally doped Bi2212 sample [8] with a  $T_c = 89$  K. In principle, at the Fermi surface ( $k = k_F$ ),  $A(\mathbf{k}, \omega)$  should have a peak centered at zero binding energy. Since ARPES only measures the occupied part of  $A$ , the ARPES spectral peak is cut off by the Fermi function, and thus its maximum is displaced to higher energy. As half of the actual spectral peak is being cut away, an estimate of its full width-half maximum (FWHM) can be obtained by doubling that of the ARPES one, yielding a value of  $\sim 200$  meV. Although quasiparticles are only expected to appear at low temperatures, we note that the peak has a width of order 2000K, well over an order of magnitude larger than the temperature, indicating that thermal broadening alone cannot be responsible for the large peak width.

We can confirm that large widths are intrinsic to *optimally* doped cuprates by examining the spectral function of the single CuO layer compound Bi2201, which has a lower  $T_c$ , and therefore a normal state accessible at a lower temperature. In curve (b) of Fig. 1 we plot ARPES data for the slightly overdoped Bi2201 compound  $Bi_{1.6}Pb_{0.4}Sr_2CuO_6$  ( $T_c = 20$  K). Even though the normal state data are now taken at 30K, the spectral width has only narrowed to a FWHM of 100 meV, and so does not exhibit a sharp quasiparticle peak. We therefore conclude that quasiparticles do not appear in the normal state of optimally doped compounds at point  $A$ , even at low temperature. As there is some evidence from transport that more Fermi liquid like behavior develops for heavily overdoped materials, the question arises whether ARPES sees evidence for normal state quasiparticles in that case. Curve (c) of Fig. 1 is a spectrum for a highly overdoped Bi2201 sample ( $T_c=4$  K) taken at a temperature of 20K. Indeed, the spectral peak is much narrower, consistent with more Fermi liquid like behavior.

Although the normal state of optimally doped cuprates does not exhibit them, quasiparticles do appear in the superconducting state of optimally doped samples at point  $A$ . Curve (d) in Fig. 1 shows a spectrum in the superconducting state, where a near resolution limited peak appears. In addition, a break clearly separates the coherent, or quasiparticle, part of the spectral function from the incoherent part, as indicated by the arrow. A significant point is that in the vicinity of the  $A$  point, the break in the spectra appears exactly at  $T_c$  [9]. This is thought to be due to the onset of superconductivity, which leads to a reduction of the scattering rate of electrons over an energy range of order 2-3 times the maximum superconducting gap [10], thus allowing quasiparticles to exist.

It is now well established that the HTSCs are *d*-wave superconductors, in which particular points along the Fermi surface (point N in the inset of Fig. 1) are characterized by nodes in the order parameter [4,5]. We now ask the question whether quasiparticles exist at these particular points –which always exhibit gapless excitations at

low temperatures. So far, it has not been possible to address this question because of resolution issues. For example, the dashed curve in the right panel of Fig. 1 shows the spectrum obtained at  $N$  with our previous momentum resolution, deep in the superconducting state ( $T=40$  K). Although this peak has been called a “quasiparticle peak” in the literature, there is no direct evidence for this in the raw data. The spectrum is as broad as the normal state spectrum of curve (a) in Fig. 1, but for a different reason. This is the direction in momentum space of largest dispersion, and the finite momentum window  $\delta k$  of the analyzer broadens the peaks as  $\delta E = \hbar v_F \delta k$ , where  $v_F$  is the Fermi velocity. From the observed dispersion, this momentum broadening can be estimated to be of order 100 meV.

Now, with a 32-fold improvement in momentum resolution (8 times along the direction normal to the Fermi surface, and 4 times in the transverse direction), we show in the solid curve of the right panel of Fig. 1 the qualitatively new result that there are true quasiparticles at the nodes of the *d*-wave superconducting state [11]. Although these data were obtained in the superconducting state, because they are at the node of the *d*-wave state, they are in fact gapless. And though the signal-to-noise ratio of the spectrum is not very high, a break separating the coherent from the incoherent part of the spectral function is visible in the lineshape as indicated by an arrow. But the converse is also true: there are no signs of quasiparticles in the normal state. Fig. 2 (left panel) shows the temperature dependence of the lineshape at point  $N$ . The lineshape above  $T_c$  is very similar to the lineshape at  $A$ , as can be seen by a direct comparison of the two in the right panel of Fig. 2. That is, the trailing edge of the spectral peak smoothly evolves into an incoherent tail going to high binding energy. As the temperature is lowered below  $T_c$ , a break begins to develop which separates the coherent quasiparticle peak from the incoherent tail.

Along  $(\pi, \pi)$ , not only is the normal state completely incoherent, but it exhibits a rather unusual lineshape with a cusp, rather than a peak, a feature observable even when the state is far from the Fermi surface. This can be seen in Fig. 3, where we plot the momentum dependence of the lineshape along the zone diagonal (at 45° to the Cu-O bond direction) in the normal (100K) and superconducting (40K) states for an optimally doped 89K sample. These spectra were taken every 0.25° (0.009 Å<sup>-1</sup>). We note the sharpening of the spectral peak in the normal state as  $k_F$  is approached, as observed before [12]. In the superconducting state, we see the new result of a coherent peak along this direction, which only exists in a narrow momentum interval about  $k_F$  ( $\pm 0.25$ °). Note that this range is a factor of 4 smaller than our previous resolution. More quantitative information can be obtained by plotting the FWHM of the spectral peak from the raw data as a function of the binding energy

of the spectral peak, as shown in Fig. 4. Above  $T_c$ , the FWHM is approximately linear in binding energy (we define the FWHM relative to the horizontal line in the right panel of Fig. 1), with a slope of 0.43. An extrapolation of the linear part to zero binding energy results in an offset of 80 meV, about an order of magnitude larger than the temperature (the decrease in the FWHM for the lowest binding energy point is due to the cut-off of the spectral peak by the Fermi function). Below  $T_c$ , the FWHM is the same as that in the normal state for binding energies above an energy of about 3 times the maximum superconducting gap ( $\Delta_{max}=25$  meV), but decreases faster than this below. The sizeable residual offset at zero binding energy is a combination of momentum and energy resolution, plus a contribution from the incoherent tail of the spectra (the FWHM of the coherent peak is 30 meV).

To make a detailed comparison to optical conductivity data would require fitting the spectra to a model self-energy, using this self-energy to construct the transport scattering rate,  $1/\tau$ , and then averaging this  $1/\tau$  over the Brillouin zone with the appropriate velocity weighting factors [13]. Rather than go through such a complicated procedure, we elect to directly compare the  $1/\tau$  data from optical conductivity in Bi2212 to the FWHM versus binding energy (discussed above), which should be a rough measure of  $1/\tau$  versus energy. This is also shown in Fig. 4. Surprisingly, at energies above  $3\Delta_{max}$ , there is a fairly good match between these two quantities, with the optical data having a slightly larger linear slope (but with about the same extrapolated offset). Below this, the optical data show a more precipitous drop, even in the normal state. The difference from ARPES is that our measurement is directly along the nodal (gapless) direction, whereas optical conductivity samples a region about the node (the region near  $(\pi, 0)$  should not contribute much to the in-plane optical conductivity because of the weak dispersion). That is, the drop seen in the optical data is due to the presence of an excitation gap (superconducting gap below  $T_c$ , pseudogap above) which does not exist along the nodal direction. Because of this, we would expect a closer correspondence with the conductivity data for ARPES data displaced away from the  $(\pi, \pi)$  direction. This is indeed the case, in that we observe a more pronounced drop in the FWHM as the momentum cuts displace away from the node direction. This is illustrated by data shown in the right panel of Fig. 4 for a cut parallel to the  $(\pi, \pi)$  direction (represented by the grey line segment in the inset of Fig. 1), with the FWHM plotted in the inset of the left panel [14]. We also observe that the break in the spectrum near  $k_F$  separating the coherent peak from the incoherent tail also occurs at the same energy, indicating a drop in the imaginary part of the self-energy at the same frequency that optical data see a drop in  $1/\tau$ . Finally, we note that the linear energy variation seen by the optical and APRES data is analogous to the linear temperature

dependence of the resistivity, ubiquitous in the cuprate superconductors, and is in support of a marginal Fermi liquid phenomenology [3].

In conclusion, we report the first observation of the intrinsic lineshape along the zone diagonal, from which we deduce a quasiparticle peak below  $T_c$  and the absence of such a peak in the normal state. The non-existence of quasiparticles in the normal state appears to be a general property of cuprate superconductors. Therefore, the formation of quasiparticles must be related to the presence of a *superconducting* state. A proper description of high temperature superconductivity will only arise after this peculiar phenomenon is understood.

This work was supported by the National Science Foundation DMR 9624048, and DMR 91-20000 through the Science and Technology Center for Superconductivity, the U. S. Dept. of Energy, Basic Energy Sciences, under contract W-31-109-ENG-38, the CREST of JST, and the Ministry of Education, Science, and Culture of Japan. The Synchrotron Radiation Center is supported by NSF DMR 9212658. JM is supported by the Swiss National Science Foundation, and MR by the Swarnajayanti fellowship of the Indian DST.

---

- [1] P. Nozieres, *Theory of interacting Fermi systems* (Addison-Wesley, Reading, 1964).
- [2] P. W. Anderson, *The Theory of Superconductivity in the High  $T_c$  Cuprates* (Princeton Univ. Press, Princeton, 1997).
- [3] C. M. Varma *et al.*, Phys. Rev. Lett. **63**, 1996 (1989).
- [4] Z.-X. Shen and D. S. Dessau, Phys. Rep. **253**, 1 (1995).
- [5] J. C. Campuzano *et al.* in *The Gap Symmetry and Fluctuations in High- $T_c$  Superconductors*, eds. J. Bok *et al.* (Plenum, New York, 1998), p. 229.
- [6] M. Randeria *et al.*, Phys. Rev. Lett. **74**, 4951 (1995).
- [7] W. N. Hardy *et al.*, Phys. Rev. Lett. **70**, 3999 (1993).
- [8] Measurements were carried out at the SRC, Wisconsin, using 22 eV photons. Samples were mounted with the  $\Gamma - X$   $(\pi, -\pi)$  direction parallel to the photon polarization, except for Fig. 1, left panel, where samples were aligned along  $\Gamma - \bar{M}$   $(\pi, 0)$ . Data were normalized to the signal above  $E_F$  (second order light) which is proportional to the photon flux, a standard procedure.
- [9] M. R. Norman *et al.*, Phys. Rev. B **57**, R11093 (1998).
- [10] M. R. Norman *et al.*, Phys. Rev. Lett. **79**, 3506 (1997).
- [11] Note the node itself is a single point, so makes a contribution of measure zero to the spectrum.
- [12] C. G. Olson *et al.*, Phys. Rev. B **42**, 381 (1990).
- [13] A. V. Puchkov, D. N. Basov, and T. Timusk, J. Phys. Cond. Matter **8**, 10049 (1996).
- [14] The spectral peaks are as sharp as the better resolution data of Fig. 3 because of the decreased dispersion away from the  $(\pi, \pi)$  direction.

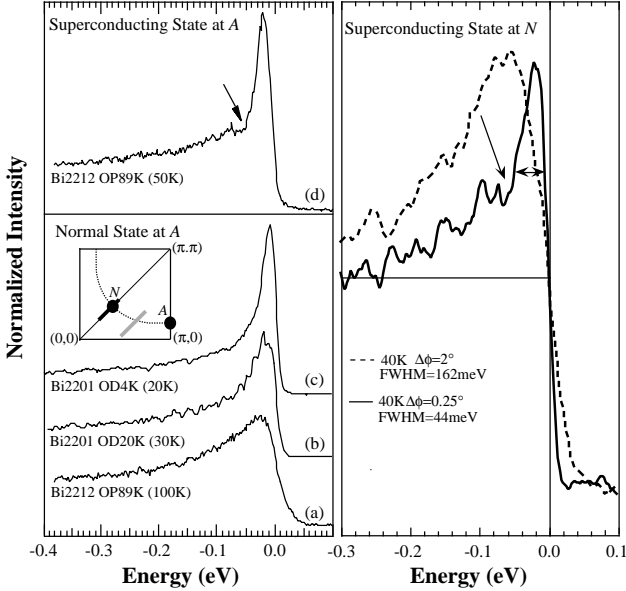


FIG. 1. Left panel: Photoemission spectra obtained at the Fermi surface at the maximum gap point (point A of the Brillouin zone inset), with spectra labelled by sample type, doping (OD for overdoped, OP for optimal doped), and onset  $T_c$ . The number in parenthesis indicates the temperature at which the spectrum was obtained. The arrow in the top panel indicates a distinct break in the lineshape. Right panel: Photoemission spectra of Bi2212 ( $T_c=89$ K) in the superconducting state at the point labelled N in the inset of Fig. 1. The spectra are labelled by the temperature at which they were taken, along with the width of the momentum window in the direction normal to the Fermi surface. Horizontal lines are used to define the FWHM plotted in Fig. 4.

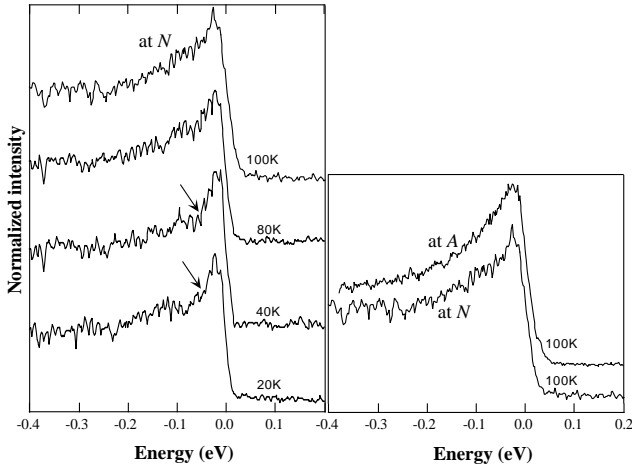


FIG. 2. Left panel: Temperature dependence of the spectra at point N in the inset of Fig. 1 for a Bi2212 sample ( $T_c=89$ K). A break in the lineshape of the spectra at 20K and 40K are indicated by arrows. Right panel: Comparison of the normal state spectra ( $T=100$ K) obtained at points A and N.

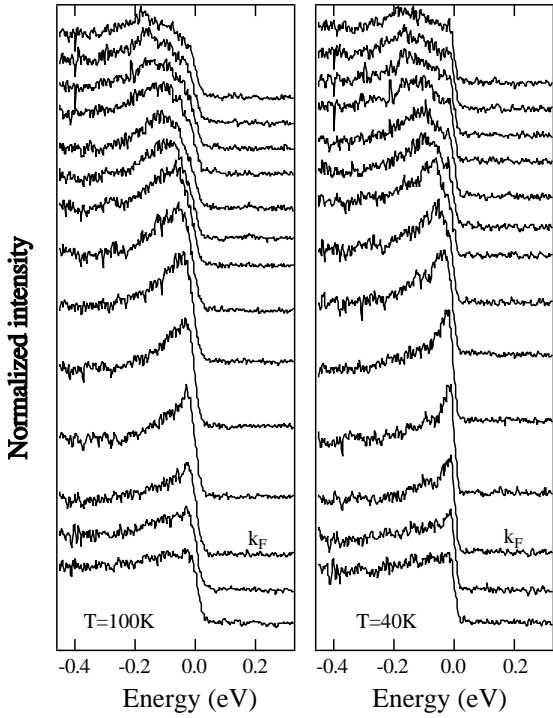


FIG. 3. Momentum dependence of the spectra of Bi2212 ( $T_c=89$ K) along the  $(\pi, \pi)$  direction -indicated by the dark line segment in the inset of Fig. 1- in the normal (100K) and superconducting (40K) states. Data were taken at intervals of  $0.25^\circ$  ( $0.009 \text{ \AA}^{-1}$ ). The spectrum corresponding to the Fermi momentum is labelled by  $k_F$ .

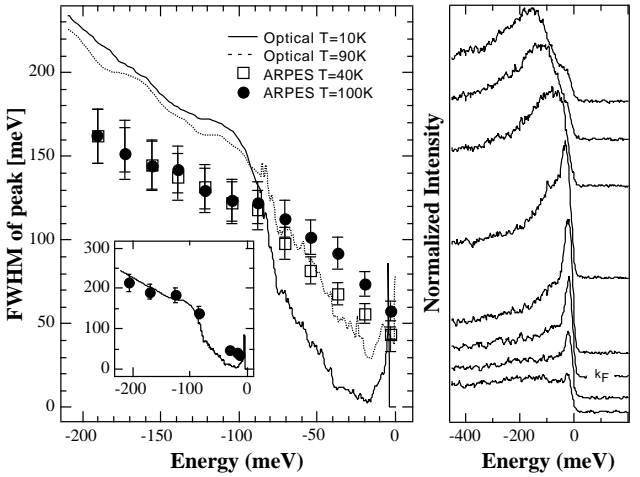


FIG. 4. Left panel: Full width-half maximum of the spectral peaks in Fig. 3 versus the binding energy of the spectral peak (symbols), and the carrier scattering rate versus energy for Bi2212 ( $T_c=90$ K) obtained from infrared reflectivity measurements (solid and dashed lines) [13]. The FWHM are defined by the horizontal lines in the right panel of Fig. 1. Right panel: Data at  $1^\circ$  steps with a  $1^\circ$  wide momentum window for a cut parallel to  $(\pi, \pi)$  (grey line segment in inset of Fig. 1). The resulting FWHM versus peak energy is shown in the inset of the left panel, along with the optical data.